

# Zero and R2D2: A Large-scale Chinese Cross-modal Benchmark and A Vision-Language Framework

Chunyu Xie<sup>1\*</sup>, Heng Cai<sup>1\*</sup>, Jianfei Song<sup>1\*</sup>, Jincheng Li<sup>1</sup>, Fanjing Kong<sup>1</sup>, Xiaoyu Wu<sup>1</sup>  
Henrique Morimitsu<sup>1,2</sup>, Lin Yao<sup>1</sup>, Dexin Wang<sup>1</sup>, Dawei Leng<sup>1</sup>, Xiangyang Ji<sup>2</sup>, Yafeng Deng<sup>1,2†</sup>

<sup>1</sup>Qihoo 360 AI Research

<sup>2</sup>Department of Automation, Tsinghua University

{xiechunyu, caiheng1, songjianfei, lijincheng, kongfanjing}@360.cn

{wuxiaoyu1, yaolin, wangdexin, lengdawei}@360.cn

henrique.morimitsu@mail.tsinghua.edu.cn

xyji@tsinghua.edu.cn

dengyafeng@gmail.com

## Abstract

Vision-language pre-training (VLP) on large-scale datasets has shown premier performance on various downstream tasks. A complete and fair benchmark (*i.e.*, including large-scale pre-training datasets and diverse downstream tasks) is essential for VLP. While there are plenty of benchmarks with English corpus, building a rich benchmark for VLP with other languages, such as Chinese, remains a critical problem. To this end, we build a large-scale Chinese cross-modal benchmark called Zero for the research community to fairly compare VLP models. We release two pre-training datasets and five fine-tuning datasets for downstream tasks. Alongside, we propose a novel pre-training framework of pre-**R**anking + **R**anking for cross-modal learning. Specifically, we apply global contrastive pre-ranking to learn the individual representations of images and texts, respectively. We then fuse the representations in a fine-grained ranking manner via an image-text cross encoder and a text-image cross encoder. To further enhance the capability of the model, we propose a two-way distillation strategy consisting of target-guided **D**istillation and feature-guided **D**istillation. For brevity, we name our model **R2D2**. We achieve state-of-the-art performance on four public cross-modal datasets and the proposed five downstream datasets. When conducting zero-shot tasks on Flickr30k-CN, COCO-CN, and MUGE, R2D2 pre-trained on a 250 million dataset achieves significant improvements of 4.7%, 5.4%, and 6.3% in mean recall compared to the state-of-the-art. The datasets, models, and codes are available at <https://github.com/yuxie11/R2D2>.

## 1 Introduction

Vision-language pre-training (VLP) mainly learns the semantic correspondence between vision and natural language. Seminal works [15, 17, 24, 26, 30] explore the VLP model and achieve significant improvement on various vision-language tasks, supported by massive data [25], excellent architectures such as Transformer [28], cross-modal models such as CLIP [24], hardware equipment, etc. In this paper, we focus on large-scale vision-language data and cross-modal learning.

With a large-scale training corpus (mainly in English language), VLP models have shown to be beneficial for downstream tasks [15, 21]. However, existing Chinese vision-language datasets are rare and with various limitations. For instance, M6-Corpus [20] is a multi-modal pre-training dataset but is still not publicly available. Wukong [9] is a newly published cross-modal pre-training dataset

with a hundred-million samples, but only retrieval tasks such as AIC-ICC [31] and MUGE [20] are considered for benchmarks there, which is not sufficient for complete evaluation of VLP on Chinese cross-modal benchmark. There are also several works that attempt to translate English cross-modal downstream datasets into Chinese like Flickr30k-CN [12]. However, they do not cover Chinese idioms and often contain errors. In this sense, how to construct a complete and fair Chinese cross-modal benchmark with high-quality Chinese descriptions is a problem yet to be solved.

In this paper, we introduce Zero, a large-scale Chinese cross-modal benchmark, containing two pre-training datasets called Zero-Corpus and five downstream datasets. Specifically, the pre-training datasets consist of one full version with 23 million image-text pairs and one smaller subset version with 2.3 million image-text pairs. The full pre-training dataset is collected from the search engine and contains images and corresponding textual descriptions, which is filtered from 5 billion image-text pairs by user click-through rate (CTR). Training VLP models on this full version may demand overwhelming GPU resources, thus a subset with 10% image-text pairs is also provided for research purpose. Along with the pre-training datasets, we provide 5 high-quality downstream datasets for both image-text retrieval and image-text matching tasks, especially featuring Flickr30k-CNA, a more comprehensive and accurate human-annotated dataset than Flickr30k-CN [12]. We build a leaderboard relying on the five downstream test datasets.

From the perspective of cross-modal learning, most existing methods [14, 17, 18, 21, 34] pay attention to exploring the association between image and text via pre-training. UNIMO [18] designs a single-stream framework to conduct pre-training tasks on a large-scale image-text dataset. CLIP [24] introduces a dual-stream based model for vision-language representation learning. However, both approaches have some drawbacks. The single-stream architecture learns coarse-grained interaction between image and text representations generated only by a few linear projectors. Meanwhile, in the dual-stream architecture, it is non-trivial to model the fine-grained associations between image and text since the corresponding representations reside in their own semantic space.

For VLP model, we propose a novel pre-training framework called R2D2 for cross-modal learning. Inspired by industrial technology such as recommender systems [3, 29] and online advertising [27], we apply global contrastive pre-ranking to obtain image-text representations and fine-grained ranking to further improve model performance. We also introduce a two-way distillation method, consisting of target-guided distillation and feature-guided distillation. The target-guided distillation increases the robustness when learning from noisy labels, while feature-guided distillation aims to improve the generalization performance of R2D2. To summarize, our main contributions are as follows:

- We propose Zero, a Chinese vision-language benchmark that includes two large-scale pre-training datasets and five downstream train/val/test sets. We correspondingly build a leaderboard to facilitate the research community making a fair comparison.
- We introduce a novel VLP framework named as **R2D2** for image-text cross-modal learning. Specifically, we propose a pre-**R**anking + **R**anking strategy to learn powerful vision-language representations and a two-way distillation method (*i.e.*, target-guided **D**istillation and feature-guided **D**istillation) to further enhance the learning capability.
- Our proposed method achieves the state-of-the-art performance on four public cross-modal datasets and the proposed five downstream datasets, showing the superior ability of our pre-trained model.

## 2 Curated VLP Benchmark: Zero

### 2.1 Pre-training Datasets

Existing public pre-training datasets suffer from two major limitations. First, the image-text pairs are collected usually by their co-occurrence relationship coarsely from third-party search engines or websites. Thus, the collected pairs are inherently noisy. Second, the text corpus lacks diversity as each image usually has one corresponding text description. To overcome these drawbacks, we curate a new dataset for Chinese image-text pre-training, called Zero-Corpus. Specifically, we extract 23 million samples from 5 billion image-text pairs collected by an image search engine. The key point is filtering the candidates by the highest user CTR, which means users have clicked the most on an image searched by the same query. Moreover, we remove inappropriate images and harmful textual descriptions to keep only the most relevant and high-quality image-text pairs. We also provide diverse textual information for each image, *i.e.*, “Title”, “Content”, and “ImageQuery”. Training

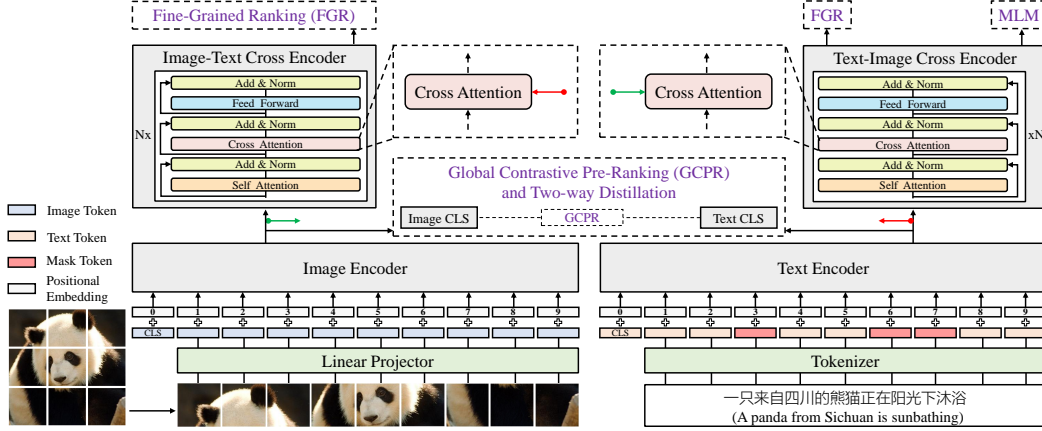


Figure 1: The overall architecture of the proposed framework. The image encoder and the text encoder aim to learn individual features of image and text, respectively. Then, the image features (green circled arrow) are fed into the text-image cross encoder. Similarly, the text features (red circled arrow) are fed into the image-text cross encoder. During pre-training, we apply global contrastive pre-ranking (GCPR) and fine-grained ranking (FGR) as pre-training objectives. Moreover, we introduce mask language modeling (MLM) and two-way distillation to obtain remarkable performance.

VLP on this full version dataset may be resource-demanding, thus we construct a smaller subset with 2.3 million image-text pairs. More details about the pre-training datasets can be found in Appendix.

## 2.2 Downstream Datasets

Compared to existing downstream datasets with English descriptions, there are fewer downstream datasets with Chinese texts. We use an image search engine to construct 4 Chinese image-text datasets, namely ICM, IQM, ICR, and IQR. In these datasets, each image has only one corresponding text. For each dataset, we divide the training set, validation set, and test set in the ratio of 8:1:1. 15 human annotators carefully label all the image-text pairs. We also translate all data of Flickr30k [35] by 6 professional Chinese and English linguists. The details of each dataset are as follows.

**Image-Caption Matching Dataset (ICM).** ICM is curated for the image-text matching task. Each image has a corresponding caption text, which describes the image in detail. We first use CTR to select the most relevant pairs. Then, human annotators manually perform a 2nd round manual correction, obtaining 400,000 image-text pairs, including 200,000 positive cases and 200,000 negative cases. We keep the ratio of positive and negative pairs consistent in each of the train/val/test sets.

**Image-Query Matching Dataset (IQM).** This is a dataset also for the image-text matching task. Different from ICM, we use the search query instead of detailed description text. In this dataset, we randomly select image-query pairs in the candidate set after performing the cleaning process described in Section 2.1. Similarly, IQM contains 200,000 positive cases and 200,000 negative cases.

**Image-Caption Retrieval Dataset (ICR).** In this dataset, we collect 200,000 image-text pairs under the rules described in ICM. It contains image-to-text retrieval and text-to-image retrieval tasks.

**Image-Query Retrieval Dataset (IQR).** IQR is also proposed for the image-text retrieval task. We randomly select 200,000 queries and the corresponding images as the annotated image-query pairs similar to IQM. We show examples of the above four datasets in Appendix.

**Flickr30k-CNA Dataset.** Former Flickr30k-CN [12] translates the training and validation sets of Flickr30k [35] using machine translation, and manually translates the test set. We check the machine-translated results and find two kinds of problems. (1) Some sentences have language problems and translation errors. (2) Some sentences have poor semantics. In addition, the different translation ways between the training set and test set prevent the model from achieving accurate performance. We gather 6 professional English and Chinese linguists to meticulously re-translate all data of Flickr30k and double-check each sentence. We name this dataset as Flickr30k-Chinese All (Flickr30k-CNA). We show some cases of the difference between Flickr30k-CN and Flickr30k-CNA in Appendix.

### 3 Approach

#### 3.1 Model Architecture

From Figure 1, R2D2 contains a text encoder, an image encoder, and two cross encoders. The text encoder and image encoder transform texts and images into sequences of hidden states separately. Then the text and image hidden states interact in the two cross encoders through cross-attention.

**Text Encoder.** We employ a BERT [5] encoder as our text encoder. Given a textual sequence, we firstly tokenize it using the tokenizer of RoBERTa-wwm-ext [4]. Here, a special  $[CLS]$  token is appended to the head of the tokenized text while a  $[SEP]$  token is appended to the tail. Then, we feed the tokenized text into the text encoder.

**Image Encoder.** For the image encoder, we adopt the Vision Transformer (ViT) [6]. We firstly rescale the input image into a standard size and split the image into patches. Each of the patches is then linearly projected and a position embedding is added. Additionally, a learnable  $[CLS]$  token is concatenated with the patch vectors. The sequential vectors are finally fed into a standard Transformer model to obtain a list of image hidden state vectors.

**Cross Encoder.** The image and text hidden vectors are fused and fed into the cross encoders. Specifically, the linear projection layer is used to change the dimensionality of each text feature and image feature to make them consistent. The multi-layer transformers fuse the feature information of both modalities with the help of cross-attention and produce the final cross-modal outputs.

#### 3.2 Pre-training Methods

We pre-train our model with three objectives. To fully explore the matching relationship between image and text pairs, we design a mechanism of pre-ranking + ranking, named global contrastive pre-ranking (GCPR) and fine-grained ranking (FGR). We adopt masked language modeling (MLM) to efficiently learn the representation of cross-modal models.

**Global Contrastive Pre-Ranking.** Traditional contrastive learning aims to align the representation of multi-modal data (e.g., paired image and text). It maximizes the similarity score of the positive pairs and minimizes the score of the negative pairs. In practice, we use global contrastive learning to accomplish the pre-ranking task. We perform full back-propagation across  $k$  GPUs. For each image  $I_i$  and the corresponding text  $T_i$ , the softmax-normalized similarity score of image-to-text and text-to-image can be defined as:

$$s(I_i, T_i) = \frac{\exp(\text{sim}(I_i, T_i)/\tau)}{\sum_{j=1}^{n \times k} \exp(\text{sim}(I_i, T_j)/\tau)}, \quad s(T_i, I_i) = \frac{\exp(\text{sim}(T_i, I_i)/\tau)}{\sum_{j=1}^{n \times k} \exp(\text{sim}(T_i, I_j)/\tau)}, \quad (1)$$

where  $n$  is the batch size of one GPU,  $k$  is the number of GPUs,  $\tau$  is a learnable temperature parameter, and  $\text{sim}(\cdot, \cdot)$  denotes the cosine similarity between a pair of image-text. Let  $\mathcal{D}$  denote the training data and  $\mathbf{y}(\cdot, \cdot)$  denote the ground-truth one-hot label. The global contrastive pre-ranking loss is calculated by the cross-entropy loss  $\mathcal{L}_c(\cdot)$ , as shown in Equation (2).

$$\mathcal{L}_{\text{GCPR}} = \frac{1}{2} \mathbb{E}_{(I, T) \sim \mathcal{D}} [\mathcal{L}_c(s(I, T), \mathbf{y}(I, T)) + \mathcal{L}_c(s(T, I), \mathbf{y}(T, I))]. \quad (2)$$

**Fine-Grained Ranking.** As aforementioned, we apply global contrastive pre-ranking to obtain the individual representations of images and texts, respectively. Relying on these representations, we next perform Fine-Grained Ranking (FGR) loss to conduct a fine-grained ranking task. To be specific, this is a binary classification task, aiming to predict whether an image-text is matched. Formally, we denote  $h_{I[CLS]}$  and  $h_{T[CLS]}$  as the output representations of two cross encoders. Given an image representation  $h_{I[CLS]}$  and a text representation  $h_{T[CLS]}$ , we feed the representations into a fully-connected layer  $g(\cdot)$  to get the predicted probabilities respectively. Let  $\mathbf{y}$  denote the ground-truth label of binary classification, we then compute the FGR loss as:

$$\mathcal{L}_{\text{FGR}} = \frac{1}{2} \mathbb{E}_{(I, T) \sim \mathcal{D}} [\mathcal{L}_c(g(h_{I[CLS]}), \mathbf{y}) + \mathcal{L}_c(g(h_{T[CLS]}), \mathbf{y})]. \quad (3)$$

**Masked Language Modeling.** We apply a masked language modeling loss to the text-image cross encoder to improve the ability to model the relationship between image and text at the token level. 15%

of the text tokens are masked in the input. All of these tokens are replaced with the  $[MASK]$  token. For the MLM task [5], the forward operations are executed individually in most VLP models [2, 15], increasing the computational cost of pre-training. In our model, the MLM task utilizes masked text and corresponding images together for denoising, which enhances the interaction between text and images. Since FGR relies heavily on this interaction ability, we propose enhanced training (ET), which integrates the MLM task into the FGR forward operations for positive image-text pairs. Experiments in Section 4.3 show that ET can reduce the computational cost of R2D2 while maintaining the accuracy of the model. For simplicity,  $\mathcal{L}_{MLM}$  denotes the loss of the MLM task.

### 3.3 Two-way Distillation

Most image-text pre-training data are collected by a semi-automatic program, which may create noisy and inaccurate samples. Imprecise labels are problematic, since they may mislead the model. To address this, we propose target-guided distillation (TgD), a teacher-student paradigm with soft targets. To further improve the generalization performance of the pre-trained model, we introduce feature-guided distillation (FgD), another teacher-student based distillation. For convenience, we call the combination of these two distillations as two-way distillation (TwD).

**Target-guided Distillation.** To decrease the risk of learning from noisy labels, we propose to adopt soft targets generated by momentum-updated encoders. Here, the momentum-updated encoder is the teacher model of distillation, which contains the exponential-moving-average weights. We combine the similarity score  $s(\cdot, \cdot)$  with one-hot labels  $\mathbf{y}(\cdot, \cdot)$  via coefficient  $\alpha$  to generate the final soft targets. Let  $\hat{\mathbf{y}}(I, T)$  and  $\hat{\mathbf{y}}(T, I)$  denote the final soft targets. Taking  $\hat{\mathbf{y}}(I, T)$  as the example, we define it as:

$$\hat{\mathbf{y}}(I, T) = \alpha s(I_m, T) + (1 - \alpha) \mathbf{y}(I, T), \quad (4)$$

where  $I_m$  represents that the images  $I$  are fed into the momentum-updated encoder. During training, we also introduce a queue mechanism and replace  $\hat{\mathbf{y}}(I, T)$  with  $\hat{\mathbf{y}}(I, T_q)$ . In practice, the text queue with a fixed size aims to maintain the recent text representations. We then concatenate the text queue and the text representations of current mini-batch to compute  $s(I_m, T_q)$  and  $\mathbf{y}(I, T_q)$ . Similarly, we perform the same process when constructing  $\hat{\mathbf{y}}(T, I_q)$ .

Considering the effectiveness of features in the queue decreases with increasing time steps, we also maintain a weighted queue  $w$  to mark the reliability of the corresponding position features. Specifically, we decay each element in the queue by a factor of 0.99 per iteration, except for the new incoming item. Further, we replace  $\mathcal{L}_c(\cdot)$  with weighted cross-entropy loss  $\mathcal{L}_w(\cdot)$  in Equation 2. With the target-guided distillation, the  $\mathcal{L}_{GCPR}^{TgD}$  is defined as:

$$\mathcal{L}_{GCPR}^{TgD} = \frac{1}{2} \mathbb{E}_{(I, T) \sim \mathcal{D}} [\mathcal{L}_w(s(I, T_q), \hat{\mathbf{y}}(I, T_q); w) + \mathcal{L}_w(s(T, I_q), \hat{\mathbf{y}}(T, I_q); w)]. \quad (5)$$

**Feature-guided Distillation.** Similar to TgD, we use a teacher-student paradigm to conduct feature-guided distillation. Taking the text encoder as the example below, the teacher character is the momentum-updated text encoder and the student is the text encoder. Here, the weights of the teacher are updated by all past text encoders via exponential-moving-average. To further improve the capability of the model, we apply a masking strategy to the inputs. In practice, we feed complete inputs into the teacher and masked inputs into the student. Relying on the momentum mechanism, we aim to make the features of the student closer to that of the teacher. Formally, the predicted distributions (*i.e.*,  $\mathcal{P}_t(T)$ ,  $\mathcal{P}_s(T)$ ) of the teacher and the student are defined as follows, respectively.

$$\mathcal{P}_t(T) = \frac{\exp((f_t(T) - \mu)/\tau_t)}{\sum_{i=1}^d \exp((f_t(T)^{(i)} - \mu^{(i)})/\tau_t)}, \quad \mathcal{P}_s(T) = \frac{\exp(f_s(T)/\tau_s)}{\sum_{i=1}^d \exp(f_s(T)^{(i)}/\tau_s)}, \quad (6)$$

where  $f_t(\cdot)$  and  $f_s(\cdot)$  denote the networks of the teacher and the student, respectively. Moreover,  $\mu$  is a momentum-updated mean of  $f_t(\cdot)$  that centers the features and  $d$  is the dimension of the features.  $\tau_t$  and  $\tau_s$  are the temperature parameters of the teacher and the student, respectively, which can sharpen the distribution of the features. Note that we do not use  $\mu$  for  $\mathcal{P}_s$  to avoid collapse in feature-guided distillation. We can obtain similar formulations for  $\mathcal{P}_s(I)$  and  $\mathcal{P}_t(I)$ . We perform the feature-guided distillation by the cross-entropy loss, and the loss  $\mathcal{L}_{FgD}$  is defined as:

$$\mathcal{L}_{FgD} = \frac{1}{2} \mathbb{E}_{(I, T) \sim \mathcal{D}} [\mathcal{L}_c(\mathcal{P}_s(I), \mathcal{P}_t(I)) + \mathcal{L}_c(\mathcal{P}_s(T), \mathcal{P}_t(T))]. \quad (7)$$

Our model is trained with the full objective:

$$\mathcal{L} = \mathcal{L}_{GCPR}^{TgD} + \mathcal{L}_{FGR} + \mathcal{L}_{FgD} + \mathcal{L}_{MLM}. \quad (8)$$

## 4 Experiments

### 4.1 Implementation Details

The number of transformer layers for the text encoder, and the two cross encoders are 12, 6, and 6, respectively. The text encoder is initialized from RoBERTa-wwm-ext [4] while the two cross encoders are randomly initialized. Following Wukong [9], we use the image encoder of 12-layers ViT-Base and 24-layers ViT-Large initialized from CLIP [24], and freeze it during pre-training. The resolution of the input image is  $224 \times 224$  in pre-training and fine-tuning. The dimension of the feature vectors of both image and text is 768. We pre-train all models with 30 epochs and fine-tune them with 10 epochs using a batchsize of 32 per GPU. We set  $\tau = 0.07$  in Equation 1,  $\tau_s = 0.1$ ,  $\tau_t = 0.04$  in Equation 6, and  $\alpha = 0.4$  in Equation 4. Moreover, the momentum is set as  $m = 0.995$ , and the queue size is 36,864. R2D2 on the 23M dataset is pre-trained with the mixed-precision technique for 4 days using 64 A100 GPUs. The pre-trained model is fine-tuned on two downstream tasks: image-text retrieval and image-text matching. More details about the fine-tuning strategy are in Appendix.

### 4.2 Comparisons with State-of-the-arts

For both image-to-text retrieval (TR) and text-to-image retrieval (IR) tasks, we report Recall@1 (R@1), Recall@5 (R@5), Recall@10 (R@10), and Mean Recall (R@M). The results of WENLAN 2.0 [8] and Wukong [9] are excerpted from their paper. From Table 2, our models outperform state-of-the-arts in most tasks, even when training with only 2.3M samples ( $\sim 2.3\%$  of Wukong data size). When pre-training on the 23M samples, we achieve even better results. Moreover, R2D2<sub>ViT-L</sub> outperforms R2D2<sub>ViT-B</sub> among all datasets. This indicates that the pre-ranking + ranking framework on our high-quality data is able to learn better fine-grained associations between image and text.

In addition, we provide the results on our proposed downstream datasets, which can be considered as baselines when using our datasets. When conducting experiments on Flickr30k-CNA, we fine-tune our pre-trained model on the training set of Flickr30k-CNA and test it on the test set of Flickr30k-CN for a fair comparison. From Table 2, R2D2 fine-tuned on Flickr30k-CNA outperforms that on Flickr30k-CN, since the quality of human-translated Flickr30k-CNA is much higher than that of machine-translated Flickr30k-CN. The performance on the test set of Flickr30k-CNA is in Appendix.

Unlike image-text retrieval, there are few datasets for the Chinese image-text matching (ITM) task. Thus, we propose image-caption matching dataset (ICM) and image-query matching dataset (IQM) for Chinese ITM task and show the corresponding results. We use Area Under Curve (AUC) as the metric. From Table 1, R2D2<sub>ViT-L</sub> achieves better results than R2D2<sub>ViT-B</sub>. Moreover, R2D2<sub>ViT-L</sub> (23M) outperforms R2D2<sub>ViT-L</sub> (2.3M) by around 4.97% and 5.68% on ICM and IQM, respectively. This implies that more Chinese high-quality data are able to improve the generalization ability of the proposed R2D2.

Table 1: Performance on ITM task.

Dataset	Method	# Pre-train Pairs	AUC
ICM	R2D2 <sub>ViT-B</sub>	2.3M	81.05
	R2D2 <sub>ViT-B</sub>	23M	86.47
	R2D2 <sub>ViT-L</sub>	2.3M	83.08
	R2D2 <sub>ViT-L</sub>	23M	88.05
	R2D2 <sub>ViT-L</sub>	250M	<b>90.60</b>
IQM	R2D2 <sub>ViT-B</sub>	2.3M	76.30
	R2D2 <sub>ViT-B</sub>	23M	82.02
	R2D2 <sub>ViT-L</sub>	2.3M	77.94
	R2D2 <sub>ViT-L</sub>	23M	83.62
	R2D2 <sub>ViT-L</sub>	250M	<b>86.71</b>

To further improve the performance, we extract 250 million image-text pairs from 5 billion samples. From Table 1 and Table 2, our models achieve the best results in various downstream tasks, which implies that increasing the data size can enhance the power of the pre-trained model.

### 4.3 Ablation Study

**Effect of Fine-Grained Ranking (FGR).** We conduct ablation studies on the 2.3 million pre-training dataset, which is a subset of Zero-Corpus. For simplicity, we define R2D2<sub>ViT-L</sub> as R2D2 in the ablation study. We first train a restricted version of R2D2 using only the global contrastive pre-ranking and the two-way distillation strategy. We denote it as PRD2. This restricted setting is conceptually similar to CLIP [24] that involves a local contrastive loss. R2D2 outperforms PRD2 in the image-text retrieval task, indicating the effectiveness of the proposed pre-ranking + ranking framework.

**Effect of Enhanced Training (ET).** In this experiment, we demonstrate the effectiveness of enhanced training. From the third row of Table 3, R2D2 (with ET) improve the recall@1 by 0.95% on image-

Table 2: Comparisons with state-of-the-art models on Image-Text Retrieval task.

Dataset	Method	# Pre-train Pairs	Image-to-Text Retrieval			Text-to-Image Retrieval			R@M
			R@1	R@5	R@10	R@1	R@5	R@10	
Flickr30k-CN	Wukong <sub>ViT-B</sub>	100M	83.9	97.6	99.0	67.6	89.6	94.2	88.7
	Wukong <sub>ViT-L</sub>	100M	92.7	99.1	99.6	77.4	94.5	97.0	93.4
	R2D2 <sub>ViT-B</sub>	2.3M	90.6	98.5	99.6	75.0	93.3	96.3	92.2
	R2D2 <sub>ViT-B</sub>	23M	92.6	99.1	99.8	78.3	94.6	97.0	93.6
	R2D2 <sub>ViT-L</sub>	2.3M	94.7	<b>99.9</b>	99.9	80.6	95.6	97.7	94.7
	R2D2 <sub>ViT-L</sub>	23M	95.0	99.7	100.0	83.4	95.9	98.1	95.4
	R2D2 <sub>ViT-L</sub>	250M	<b>95.6</b>	99.8	<b>100.0</b>	<b>84.4</b>	<b>96.7</b>	<b>98.4</b>	<b>95.8</b>
COCO-CN	Wukong <sub>ViT-B</sub>	100M	65.8	90.3	96.6	67.0	91.4	96.7	84.6
	Wukong <sub>ViT-L</sub>	100M	73.3	94.0	98.0	74.0	94.4	98.1	88.6
	R2D2 <sub>ViT-B</sub>	2.3M	68.6	92.9	97.8	67.9	93.4	97.0	86.3
	R2D2 <sub>ViT-B</sub>	23M	76.1	95.3	98.5	75.1	94.2	98.1	89.6
	R2D2 <sub>ViT-L</sub>	2.3M	74.1	94.3	98.7	72.9	94.5	98.1	88.8
	R2D2 <sub>ViT-L</sub>	23M	77.4	96.3	98.7	78.1	95.3	98.5	90.7
	R2D2 <sub>ViT-L</sub>	250M	<b>79.3</b>	<b>97.1</b>	<b>98.7</b>	<b>79.1</b>	<b>96.5</b>	<b>98.9</b>	<b>91.6</b>
AIC-ICC	WenLan 2.0	650M	45.6	68.0	76.3	34.1	58.9	69.1	58.7
	Wukong <sub>ViT-B</sub>	100M	47.5	70.6	78.6	36.7	56.7	71.7	57.0
	Wukong <sub>ViT-L</sub>	100M	61.6	80.5	<b>86.1</b>	48.6	72.5	80.2	71.6
	R2D2 <sub>ViT-B</sub>	2.3M	52.6	74.0	80.8	44.1	71.2	79.1	67.0
	R2D2 <sub>ViT-B</sub>	23M	55.9	76.0	82.1	47.1	72.8	80.5	69.1
	R2D2 <sub>ViT-L</sub>	2.3M	63.4	80.5	84.9	55.8	77.7	83.0	74.2
	R2D2 <sub>ViT-L</sub>	23M	64.4	80.4	85.0	56.8	78.2	<b>83.6</b>	74.7
	R2D2 <sub>ViT-L</sub>	250M	<b>65.4</b>	<b>80.3</b>	84.7	<b>57.3</b>	<b>78.1</b>	83.0	<b>74.8</b>
MUGE	Wukong <sub>ViT-B</sub>	100M	-	-	-	39.2	66.9	77.4	61.2
	Wukong <sub>ViT-L</sub>	100M	-	-	-	52.7	77.9	85.6	72.1
	R2D2 <sub>ViT-B</sub>	2.3M	-	-	-	36.8	65.9	78.1	60.3
	R2D2 <sub>ViT-B</sub>	23M	-	-	-	47.4	75.1	83.5	68.7
	R2D2 <sub>ViT-L</sub>	2.3M	-	-	-	45.8	72.7	82.5	67.0
	R2D2 <sub>ViT-L</sub>	23M	-	-	-	53.8	79.6	86.9	73.4
	R2D2 <sub>ViT-L</sub>	250M	-	-	-	<b>60.1</b>	<b>82.9</b>	<b>89.4</b>	<b>77.5</b>
Flickr30k-CNA	R2D2 <sub>ViT-B</sub>	2.3M	91.7	98.9	99.6	76.0	93.5	96.3	92.7
	R2D2 <sub>ViT-B</sub>	23M	93.2	99.4	99.7	79.6	95.2	97.5	94.1
	R2D2 <sub>ViT-L</sub>	2.3M	95.4	<b>99.9</b>	99.9	82.2	96.2	98.0	95.3
	R2D2 <sub>ViT-L</sub>	23M	96.5	99.7	<b>100.0</b>	83.6	96.5	98.4	95.8
	R2D2 <sub>ViT-L</sub>	250M	<b>96.9</b>	99.8	<b>100.0</b>	<b>84.9</b>	<b>97.0</b>	<b>98.6</b>	<b>96.2</b>
ICR	R2D2 <sub>ViT-B</sub>	2.3M	28.8	55.0	65.9	27.9	54.0	65.2	49.5
	R2D2 <sub>ViT-B</sub>	23M	43.4	69.8	78.4	42.2	69.4	77.8	63.5
	R2D2 <sub>ViT-L</sub>	2.3M	35.4	62.0	72.0	34.8	61.5	71.8	56.3
	R2D2 <sub>ViT-L</sub>	23M	50.6	76.0	82.9	50.1	75.7	82.7	69.6
	R2D2 <sub>ViT-L</sub>	250M	<b>61.5</b>	<b>82.9</b>	<b>87.7</b>	<b>60.7</b>	<b>82.0</b>	<b>86.9</b>	<b>77.0</b>
IQR	R2D2 <sub>ViT-B</sub>	2.3M	18.7	41.0	52.0	17.7	40.0	51.3	36.8
	R2D2 <sub>ViT-B</sub>	23M	27.9	54.5	64.4	27.4	53.4	63.6	48.5
	R2D2 <sub>ViT-L</sub>	2.3M	22.4	47.2	57.9	22.1	46.1	57.2	42.1
	R2D2 <sub>ViT-L</sub>	23M	32.9	59.8	69.6	32.6	59.2	68.6	53.8
	R2D2 <sub>ViT-L</sub>	250M	<b>41.9</b>	<b>67.8</b>	<b>75.9</b>	<b>41.3</b>	<b>67.6</b>	<b>75.4</b>	<b>61.7</b>

to-text retrieval task. Another advantage is that R2D2 uses less computational resources than R2D2 w/o ET. R2D2 requires 154.0 GFLOPs and can run at 1.4 iterations per second (Iter/s), while without ET we get 168.8 GFLOPs and 1.1 Iter/s. Moreover, the AUC is increased from 80.27% to 80.51% when ET is applied to the training procedure. This indicates that ET is able to both reduce the computational cost of R2D2 and improve the capability of the learning process.

**Effect of Two-way Distillation (TwD).** The proposed two-way distillation is composed of target-guided distillation (TgD) and feature-guided distillation (FgD). When removing TwD, the R@M decreases from 74.06% to 73.10%, and the AUC from 80.51% to 80.31%. By analyzing the two components of TwD, we see that performing feature alignment is important, since the model w/o FgD shows a more noticeable drop in performance. Although milder, removing TgD also causes a

Table 3: Effect of different components of R2D2. Note that we conduct ablation studies and report the average results on all downstream datasets for image-text retrieval and image-text matching tasks.

Method	Image-to-Text Retrieval			Text-to-Image Retrieval			R@M	AUC
	R@1	R@5	R@10	R@1	R@5	R@10		
PRD2	53.61	75.13	81.60	43.62	70.79	79.88	66.71	-
R2D2	<b>64.20</b>	<b>80.63</b>	<b>85.55</b>	<b>56.23</b>	<b>77.81</b>	<b>84.06</b>	<b>74.06</b>	<b>80.51</b>
R2D2 w/o ET	63.25	78.49	85.09	55.56	77.42	83.08	73.53	80.27
R2D2 w/o TwD	63.19	79.62	84.91	54.85	76.77	83.58	73.10	80.31
R2D2 w/o TgD	63.98	80.59	85.50	56.13	77.29	83.44	73.71	80.42
R2D2 w/o FgD	63.47	79.99	85.24	55.05	76.98	83.63	73.29	80.40

Table 4: Zero-shot results of different methods on downstream Chinese image-text datasets.

Dataset	Method	# Pre-train Pairs	Image-to-Text Retrieval			Text-to-Image Retrieval			R@M	AUC
			R@1	R@5	R@10	R@1	R@5	R@10		
Flickr30k-CN	Wukong <sub>VIT-L</sub>	100M	76.1	94.8	97.5	51.7	78.9	86.3	80.9	-
	R2D2 <sub>VIT-L</sub>	23M	70.2	94.1	97.6	55.9	83.5	90.6	82.0	-
	R2D2 <sub>VIT-L</sub>	250M	77.6	96.7	98.9	60.9	86.8	92.7	<b>85.6</b>	-
COCO-CN	Wukong <sub>VIT-L</sub>	100M	55.2	81.0	90.6	53.4	80.2	90.1	75.1	-
	R2D2 <sub>VIT-L</sub>	23M	58.1	86.8	93.3	55.0	83.1	92.5	78.1	-
	R2D2 <sub>VIT-L</sub>	250M	63.3	89.3	95.7	56.4	85.0	93.1	<b>80.5</b>	-
MUGE	Wukong <sub>VIT-L</sub>	100M	-	-	-	42.7	69.0	78.0	63.2	-
	R2D2 <sub>VIT-L</sub>	23M	-	-	-	41.0	67.8	76.6	61.8	-
	R2D2 <sub>VIT-L</sub>	250M	-	-	-	49.5	75.7	83.2	<b>69.5</b>	-
AIC-ICC	R2D2 <sub>VIT-L</sub>	23M	22.0	36.8	42.1	10.6	21.7	27.0	26.7	-
	R2D2 <sub>VIT-L</sub>	250M	30.7	47.2	52.9	14.9	28.1	33.4	<b>34.5</b>	-
ICR	R2D2 <sub>VIT-L</sub>	23M	46.8	72.6	79.3	44.6	70.2	76.0	64.9	-
	R2D2 <sub>VIT-L</sub>	250M	58.0	80.5	85.2	55.9	78.2	82.4	<b>73.4</b>	-
IQR	R2D2 <sub>VIT-L</sub>	23M	31.7	58.1	67.1	30.0	54.8	62.1	50.6	-
	R2D2 <sub>VIT-L</sub>	250M	38.4	64.8	72.8	37.4	62.6	69.0	<b>57.5</b>	-
ICM	R2D2 <sub>VIT-L</sub>	23M	-	-	-	-	-	-	-	87.4
	R2D2 <sub>VIT-L</sub>	250M	-	-	-	-	-	-	-	<b>90.5</b>
IQM	R2D2 <sub>VIT-L</sub>	23M	-	-	-	-	-	-	-	81.8
	R2D2 <sub>VIT-L</sub>	250M	-	-	-	-	-	-	-	<b>84.7</b>

reduction in performance. These results indicate that both components are relevant and TwD is an effective way to improve the generalization performance of the pre-trained model.

#### 4.4 Further Experiments

**Zero-shot Tasks.** To demonstrate the generalization performance of our method, we conduct zero-shot transfer experiments. From Table 4, compared with current state-of-the-art Wukong<sub>VIT-L</sub>, our R2D2<sub>VIT-L</sub> pre-trained on the 23 million dataset achieves comparable or even better performance on Flickr30k-CN, COCO-CN, and MUGE with much less pre-training data. Moreover, R2D2<sub>VIT-L</sub> pre-trained on the 250 million dataset (250M) shows the powerful results, increasing 4.7%, 5.4%, and 6.3% in R@M respectively. We show more results on our proposed downstream datasets *i.e.*, ICR, IQR, ICM, and IQM. Note that the results of R2D2<sub>VIT-L</sub> on Flickr30k-CN are the same as that on Flickr30k-CN since we use the same test set for a fair comparison as described in Section 4.2. In this way, we do not report the results of R2D2<sub>VIT-L</sub> on Flickr30k-CNA.

**Entity-conditioned Image Visualization.** In this experiment, we attempt to visualize the attention map of images on COCO-CN. Specifically, we first extract an entity from the Chinese text and calculate the attention score of an image-entity pair. Here, we select the third layer of the text-image cross encoder following [15]. Figure 2 illustrates the visual explanations of four images over four different entities. It shows that R2D2 learns well to align text with the correct content inside the image. More analysis is shown in Appendix.





Figure 2: Entity-conditioned image visualization.

## 5 Related Work

### 5.1 Vision-Language Datasets

Chinese vision-language benchmark requires images and high-quality Chinese texts, which are hard to obtain and still rare for the research community’s reach. To this end, existing public datasets [12, 19] use machine translation to adapt their English versions [1, 35] to Chinese, but the data quality is sacrificed due to machine translation errors. Newly reported datasets with Chinese texts [8, 9, 20] are proposed for Chinese VLP. However, they are either not publicly available or lack sufficient downstream tasks. In this paper, we propose a Chinese vision-language benchmark that covers two large-scale pre-training datasets and five high-quality downstream datasets.

### 5.2 Vision-Language Pre-training Learning

**Vision-Language Architecture.** The vision-language pre-training architectures can be categorized as: single-stream and dual-stream. Most existing single-stream models [2, 13, 17, 22, 23] concatenate image and text as a single input to model the interactions between image and text within a transformer model [28]. On the other hand, popular dual-stream models [7, 11, 16, 21, 24, 30] aim to align image and text into a unified semantic space via contrastive learning. Besides, some works [14, 15] align the individual features of images and texts in a dual-stream architecture, and then fuse the features in a unified semantic space via a single-stream architecture. However, they ignore supervised signals from images. In addition, they use traditional masked language modeling (MLM) and local contrastive learning to conduct pre-training tasks, leading to potential inferior model performance. In this paper, we explore the effective signals via an image-text cross encoder and a text-image cross encoder while also maintaining the bottom dual-stream architecture. Moreover, we improve MLM with enhanced training and apply global contrastive learning to further improve performance.

**Knowledge Distillation.** The general purpose of knowledge distillation is to improve the student model’s performance by simulating the output of the teacher network [10, 32, 36]. Compared to previous works [15, 33, 36], we propose target-guided distillation with a weighted momentum queue and feature-guided distillation to stabilize the model representations for vision-language pre-training.

## 6 Conclusion and Social Impacts

In this paper, we propose a Chinese vision-language benchmark called Zero. We introduce a novel vision-language method, namely R2D2. R2D2 adopts a framework of pre-ranking + ranking for cross-modal learning. To alleviate the risk from noise and improve the model capability, we propose a two-way distillation strategy. We achieve state-of-the-art results on four public downstream datasets and our five downstream datasets. A limitation of our method is that it only treats Chinese text and there is no experiment in English. We will adopt R2D2 to English VLP learning in future work.

We will release all datasets and models. We expect that the good cross-modal benchmark and framework will encourage a plethora of engineers to develop more effective methods in specific real-world scenarios, such as searching images by texts. While the benchmark and framework promise positive impacts, abuse can never be avoided, causing unwanted social implications.

## References

- [1] X. Chen, H. Fang, T.-Y. Lin, R. Vedantam, S. Gupta, P. Dollar, and C. L. Zitnick. Microsoft coco captions: Data collection and evaluation server, 2015.
- [2] Y.-C. Chen, L. Li, L. Yu, A. El Kholy, F. Ahmed, Z. Gan, Y. Cheng, and J. Liu. Uniter: Universal image-text representation learning. In *European conference on computer vision*, pages 104–120. Springer, 2020.
- [3] H.-T. Cheng, L. Koc, J. Harmsen, T. Shaked, T. Chandra, H. Aradhye, G. Anderson, G. Corrado, W. Chai, M. Ispir, et al. Wide & deep learning for recommender systems. In *Proceedings of the 1st workshop on deep learning for recommender systems*, pages 7–10, 2016.
- [4] Y. Cui, W. Che, T. Liu, B. Qin, S. Wang, and G. Hu. Revisiting pre-trained models for chinese natural language processing. *arXiv preprint arXiv:2004.13922*, 2020.
- [5] J. Devlin, M.-W. Chang, K. Lee, and K. Toutanova. Bert: Pre-training of deep bidirectional transformers for language understanding, 2018.
- [6] A. Dosovitskiy, L. Beyer, A. Kolesnikov, D. Weissenborn, X. Zhai, T. Unterthiner, M. Dehghani, M. Minderer, G. Heigold, S. Gelly, et al. An image is worth 16x16 words: Transformers for image recognition at scale. *arXiv preprint arXiv:2010.11929*, 2020.
- [7] F. Faghri, D. J. Fleet, J. R. Kiros, and S. Fidler. Vse++: Improving visual-semantic embeddings with hard negatives, 2017.
- [8] N. Fei, Z. Lu, Y. Gao, G. Yang, Y. Huo, J. Wen, H. Lu, R. Song, X. Gao, T. Xiang, H. Sun, and J.-R. Wen. Wenlan 2.0: Make ai imagine via a multimodal foundation model, 2021.
- [9] J. Gu, X. Meng, G. Lu, L. Hou, M. Niu, H. Xu, X. Liang, W. Zhang, X. Jiang, and C. Xu. Wukong: 100 million large-scale chinese cross-modal pre-training dataset and a foundation framework. *arXiv preprint arXiv:2202.06767*, 2022.
- [10] G. E. Hinton, O. Vinyals, and J. Dean. Distilling the knowledge in a neural network. *arXiv: Machine Learning*, 2015.
- [11] C. Jia, Y. Yang, Y. Xia, Y.-T. Chen, Z. Parekh, H. Pham, Q. Le, Y.-H. Sung, Z. Li, and T. Duerig. Scaling up visual and vision-language representation learning with noisy text supervision. In *International Conference on Machine Learning*, pages 4904–4916. PMLR, 2021.
- [12] W. Lan, X. Li, and J. Dong. Fluency-guided cross-lingual image captioning. In *Proceedings of the 25th ACM international conference on Multimedia*, pages 1549–1557, 2017.
- [13] G. Li, N. Duan, Y. Fang, M. Gong, D. Jiang, and M. Zhou. Unicoder-vl: A universal encoder for vision and language by cross-modal pre-training, 2019.
- [14] J. Li, D. Li, C. Xiong, and S. Hoi. Blip: Bootstrapping language-image pre-training for unified vision-language understanding and generation, 2022.
- [15] J. Li, R. R. Selvaraju, A. D. Gotmare, S. Joty, C. Xiong, and S. Hoi. Align before fuse: Vision and language representation learning with momentum distillation. In *NeurIPS*, 2021.
- [16] K. Li, Y. Zhang, K. Li, Y. Li, and Y. Fu. Visual semantic reasoning for image-text matching. In *Proceedings of the IEEE/CVF International conference on computer vision*, pages 4654–4662, 2019.
- [17] L. H. Li, M. Yatskar, D. Yin, C.-J. Hsieh, and K.-W. Chang. Visualbert: A simple and performant baseline for vision and language, 2019.
- [18] W. Li, C. Gao, G. Niu, X. Xiao, H. Liu, J. Liu, H. Wu, and H. Wang. Unimo: Towards unified-modal understanding and generation via cross-modal contrastive learning. 12 2020.
- [19] X. Li, C. Xu, X. Wang, W. Lan, Z. Jia, G. Yang, and J. Xu. Coco-cn for cross-lingual image tagging, captioning, and retrieval. *IEEE Transactions on Multimedia*, 21(9):2347–2360, 2019.
- [20] J. Lin, R. Men, A. Yang, C. Zhou, M. Ding, Y. Zhang, P. Wang, A. Wang, L. Jiang, X. Jia, et al. M6: A chinese multimodal pretrainer. *arXiv preprint arXiv:2103.00823*, 2021.
- [21] J. Lu, D. Batra, D. Parikh, and S. Lee. Vilbert: Pretraining task-agnostic visiolinguistic representations for vision-and-language tasks, 2019.

- [22] J. Lu, V. Goswami, M. Rohrbach, D. Parikh, and S. Lee. 12-in-1: Multi-task vision and language representation learning, 2019.
- [23] D. Qi, L. Su, J. Song, E. Cui, T. Bharti, and A. Sacheti. Imagebert: Cross-modal pre-training with large-scale weak-supervised image-text data, 2020.
- [24] A. Radford, J. W. Kim, C. Hallacy, A. Ramesh, G. Goh, S. Agarwal, G. Sastry, A. Askell, P. Mishkin, J. Clark, G. Krueger, and I. Sutskever. Learning transferable visual models from natural language supervision, 2021.
- [25] C. Schuhmann, R. Vencu, R. Beaumont, R. Kaczmarczyk, C. Mullis, A. Katta, T. Coombes, J. Jitsev, and A. Komatsuzaki. LAION-400M: open dataset of clip-filtered 400 million image-text pairs. *CoRR*, abs/2111.02114, 2021.
- [26] A. Singh, R. Hu, V. Goswami, G. Couairon, W. Galuba, M. Rohrbach, and D. Kiela. Flava: A foundational language and vision alignment model. *arXiv preprint arXiv:2112.04482*, 2021.
- [27] S. Tan, M. Li, W. Zhao, Y. Zheng, X. Pei, and P. Li. Multi-task and multi-scene unified ranking model for online advertising. In *2021 IEEE International Conference on Big Data (Big Data)*, pages 2046–2051. IEEE, 2021.
- [28] A. Vaswani, N. Shazeer, N. Parmar, J. Uszkoreit, L. Jones, A. N. Gomez, L. Kaiser, and I. Polosukhin. Attention is all you need. 6 2017.
- [29] Z. Wang, L. Zhao, B. Jiang, G. Zhou, X. Zhu, and K. Gai. Cold: Towards the next generation of pre-ranking system. *arXiv preprint arXiv:2007.16122*, 2020.
- [30] F. Wei, Y. Gao, Z. Wu, H. Hu, and S. Lin. Aligning pretraining for detection via object-level contrastive learning, 2021.
- [31] J. Wu, H. Zheng, B. Zhao, Y. Li, B. Yan, R. Liang, W. Wang, S. Zhou, G. Lin, Y. Fu, Y. Wang, and Y. Wang. Ai challenger : A large-scale dataset for going deeper in image understanding, 2017.
- [32] Q. Xie, M.-T. Luong, E. Hovy, and Q. V. Le. Self-training with noisy student improves imagenet classification. *computer vision and pattern recognition*, 2020.
- [33] Y. Xu, X. Qiu, L. Zhou, and X. Huang. Improving BERT fine-tuning via self-ensemble and self-distillation. *CoRR*, abs/2002.10345, 2020.
- [34] L. Yao, R. Huang, L. Hou, G. Lu, M. Niu, H. Xu, X. Liang, Z. Li, X. Jiang, and C. Xu. Filip: Fine-grained interactive language-image pre-training. *arXiv preprint arXiv:2111.07783*, 2021.
- [35] P. Young, A. Lai, M. Hodosh, and J. Hockenmaier. From image descriptions to visual denotations: New similarity metrics for semantic inference over event descriptions. *Transactions of the Association for Computational Linguistics*, 2:67–78, 2014.
- [36] K. Yue, J. Deng, and F. Zhou. Matching guided distillation. *europaean conference on computer vision*, 2020.

---

## Appendix

---

### A Details of Zero-Corpus

We illustrate several representative examples of Zero-Corpus in Figure A. Each sample contains one image and its corresponding attributes. For ease of understanding, we add an English translation version after each Chinese text. There are 3 types of text fields associated with each image: “Title”, “Content” and “ImageQuery”. “Title” and “Content” come from the source webpage containing the image, and the latter is also termed as surrounding text in other works. “ImageQuery” is the associated query string for the corresponding image. The average length of “Title”, “Content”, and “ImageQuery” is 5, 18, and 29, respectively. During pre-training, we randomly select one from the 3 text fields to construct an image-text pair, ensuring the data diversity. In this way, the pre-trained model can flexibly fit different text lengths on various downstream tasks. For instance, the text length of AIC-ICC is about 18 words while the text length of MUGE is less than 10 words.

We apply a series of filtering strategies to construct the Zero-Corpus. For images, we filter out images with both dimensions smaller than 100 pixels or aspect ratio out of the range  $[1/4, 4]$ . In addition, we filter images that contain sensitive information, such as sexual, violent scenes, etc. For texts, we remove texts shorter than 2 words or longer than 128 words. Also, we remove texts that contain sensitive as in image filtering. We hope this dataset will bring help to the research community.

### B Examples of the Proposed Downstream Datasets

We illustrate examples of ICM, IQM, ICM, and IQR in Figure B. Moreover, Figure C highlights some cases of the difference between Flickr30k-CN and our proposed Flickr30k-CNA.

### C Details of Fine-tuning Strategy

**Fine-tuning Strategy of Image-Text retrieval.** We jointly optimize the GCPR loss (Equation 2) and the FGR loss (Equation 3). We extract the individual features of images and texts via our dual-stream encoder and compute the similarity of all image-text pairs. Then we take the top-K candidates and use two cross encoders to further calculate the corresponding similarity scores for ranking during inference. We use a mean operation for the outputs of the two cross encoders. Here, we adjust the K on different downstream datasets. We fine-tune the pre-trained model on 7 downstream datasets, including Flickr30k-CN, COCO-CN, AIC-ICC, MUGE, ICR, IQR, and Flickr30k-CNA. K is set as 128, 256, 32, 64, 64, 64, 128, respectively.

For both image-to-text retrieval (TR) and text-to-image retrieval (IR) tasks, we report Recall@1 (R@1), Recall@5 (R@5), Recall@10 (R@10), and Mean Recall (R@M). For AIC-ICC and MUGE, we report their results on the validation sets, since their test sets are not released. For ICR and IQR, we also report the results on the validation sets in this paper, since we use the corresponding test sets to build a leaderboard. The test set of Flickr30k-CNA is also added to the leaderboard. For Flickr30k-CNA, we show the performance on the test set of Flickr30k-CN for a fair comparison in the main paper. Besides, we show more results on the test set of Flickr30k-CNA to demonstrate the superiority of our manually labeled dataset in Section E of Appendix. For the remaining downstream datasets, we report the results on the test sets. Following [9], we select the first 10,000 images with the corresponding 50,000 texts when testing on AIC-ICC. In particular, we only provide IR scores on MUGE since it only has IR settings.

**Fine-tuning Strategy of Image-Text Matching.** This task predicts whether an image-text pair is matched or not. During fine-tuning, we only apply the FGR loss (Equation 3). Additionally, we report the results on the validation sets of ICM and IQM. The statistics of all downstream datasets are also present in Table A.

	<p><b>Title:</b> 五大地缝奇观欣赏 (View of the five fissure wonders)</p> <p><b>Content:</b> 奉节地缝亦称天井峡地缝, 全长有37公里, 最大深度有229米, 而最窄处仅2米、而峡谷高度达900米, 形成气势宏伟的“一线天”, 被岩溶专家称作“世界喀斯特峡谷奇中之稀”。峡谷上段较为开阔, 但愈往下愈狭窄, 上部宽10至30米, 谷底宽仅1至30米, 悬崖最深处达300米</p> <p>(Fengjie fissure, also known as Tianjingxia fissure, has a total length of 37 kilometers and a maximum depth of 229 meters. The narrowest point is only 2 meters and the height of the canyon is 900 meters, forming a magnificent "one-line sky". The Fengjie fissure is called "the rarest karst canyon in the world" by karst experts. The upper part of the fissure is relatively open, but it becomes narrower as it goes down. The upper part is 10 to 30 meters wide, the bottom of the valley is only 1 to 30 meters wide, and the deepest cliff is 300 meters.)</p> <p><b>ImageQuery:</b> 天井峡地缝 (TianJingXia fissure)</p> <p><b>ImageUrl:</b> <a href="https://n.sinaimg.cn/sinakd20200518ac/219/w490h529/20200518/b5dc-itvqcaz9771277.jpg">https://n.sinaimg.cn/sinakd20200518ac/219/w490h529/20200518/b5dc-itvqcaz9771277.jpg</a></p>
	<p><b>Title:</b> 游览大沼国立公园, 这里山清水秀白云蓝天, 大沼、小沼、莼菜沼三个高山湖皆属于大沼国定公园 (Onuma National Park is with clear waters, white clouds and a blue sky. All three alpine lakes (i.e., Onuma, Konuma, and Uzbekistan) belong to Onuma National Park.)</p> <p><b>Content:</b> 游览大沼国立公园, 这里山清水秀白云蓝天, 大沼、小沼、莼菜沼三个高山湖皆属于大沼国定公园。大沼是由驹岳火山喷发后生成的面积24平方公里的湖泊, 有大小126个岛屿、32湖湾所组成, 这些岛屿由18座桥梁连接的景象十分秀美, 富有欧洲风味的风景。</p> <p>(Onuma National Park is with clear waters, white clouds and a blue sky. All three alpine lakes (i.e., Onuma, Konuma, and Uzbekistan) belong to Onuma National Park. Onuma is a lake with an area of 24 square kilometers formed after the eruption of the Komagatake volcano. It consists of 126 islands and 32 bays. The view of these islands connected by 18 bridges is very beautiful, full of European-style scenery.)</p> <p><b>ImageQuery:</b> 蓝天山清水秀 (Blue sky, beautiful scenery)</p> <p><b>ImageUrl:</b> <a href="https://img1.qunarzz.com/travel/d5/1510/fb/7336bbdc82ce34f7.jpg_r_720x480x95_8bdc811.jpg">https://img1.qunarzz.com/travel/d5/1510/fb/7336bbdc82ce34f7.jpg_r_720x480x95_8bdc811.jpg</a></p>
	<p><b>Title:</b> 英宠物狗戴墨镜穿潮装, 百变时装造型受热捧 (British pet dogs wear sunglasses and trendy clothes. The ever-changing fashion styles are popular.)</p> <p><b>Content:</b> 一只名叫托斯特(Toast)的查尔斯王小猎犬不用拥有专属于自己的漂亮手提包</p> <p>(A King Charles Spaniel named Toast doesn't have its own fancy handbag.)</p> <p><b>ImageQuery:</b> 戴墨镜的狗, 戴墨镜的人, 狗戴墨镜, 墨镜狗狗, 戴墨镜的狗狗图片, 宠物戴墨镜, 漂亮的宠物狗造型, 宠物戴墨镜和围巾, 橙色的宠物狗, 小猎犬戴墨镜, 舔脚, 时装造型, 狗狗舔脚, 小狗戴墨镜, 狗狗戴墨镜 (Dog with sunglasses)</p> <p><b>ImageUrl:</b> <a href="http://www.people.com.cn/mediafile/pic/20140610/32/6255024078836657304.jpg">http://www.people.com.cn/mediafile/pic/20140610/32/6255024078836657304.jpg</a></p>
	<p><b>Title:</b> 猴子捞月 (Monkey fishing for the moon)</p> <p><b>Content:</b> 猴子捞月 (Monkey fishing for the moon)</p> <p><b>ImageQuery:</b> 猴子捞月 (Monkey fishing for the moon)</p> <p><b>ImageUrl:</b> <a href="https://youer.chazidian.com/uploadfile/image/20121114/3921c63abc1decc364602880cb88c962.jpg">https://youer.chazidian.com/uploadfile/image/20121114/3921c63abc1decc364602880cb88c962.jpg</a></p>
	<p><b>Title:</b> 零基础学绘画-彩铅《紫红色百合花》 (Zero Basic Learning Painting - Color Lead "Fuchsia Lily")</p> <p><b>Content:</b> 最终的效果如图, 能出这样的效果, 真的是一层层涂出来的 (The final view is shown in the figure. To achieve such a view, it is painted layer by layer.)</p> <p><b>ImageQuery:</b> 彩铅百合, 彩铅百合绘画大全 (Color lead lily, color lead lily painting Daquan)</p> <p><b>ImageUrl:</b> <a href="http://5b0988e595225.cdn.sohucs.com/q_70,c_zoom,w_640/images/20180404/aff256df13914b918522acf6094856d.jpeg">http://5b0988e595225.cdn.sohucs.com/q_70,c_zoom,w_640/images/20180404/aff256df13914b918522acf6094856d.jpeg</a></p>
	<p><b>Title:</b> 宾夕法尼亚州立大学(The Pennsylvania State University)</p> <p><b>Content:</b> 宾夕法尼亚州立大学(The Pennsylvania State University)</p> <p><b>ImageQuery:</b> 宾夕法尼亚大学校徽, 宾州州立大学 (The school badge of The Pennsylvania State University, The Pennsylvania State University)</p> <p><b>ImageUrl:</b> <a href="http://pic.baike.soso.com/p/20140414/bki-20140414115942-921021200.jpg">http://pic.baike.soso.com/p/20140414/bki-20140414115942-921021200.jpg</a></p>

Figure A: Examples of Zero-Corpus.



Figure B: Image-text examples of ICM, IQM, ICR and IQR from left to right.

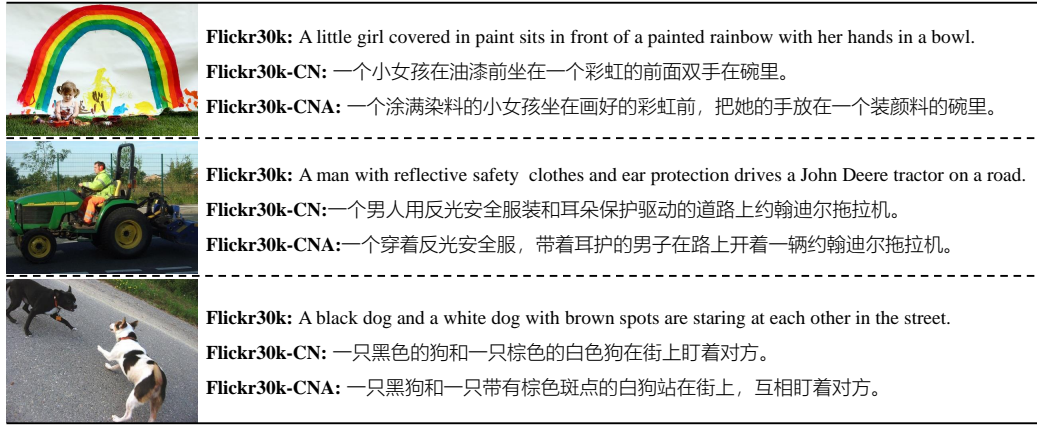


Figure C: Comparisons of Flickr30k, Flickr30k-CN and our proposed Flickr30k-CNA.

Table A: Statistics and comparison of different datasets.

Dateset	#Image/#Text		
	Train	Val	Test
Flickr30k-CN [12]	29.7K/148.9K	1K/5K	1K/5K
COCO-CN [19]	18.3K/20K	1K/1.1K	1K/1K
AIC-ICC [31]	210K/1.05M	30K/150K	30K/150K
MUGE [20]	129.4K/248.8K	29.8K/5K	30.4K/5K
ICM	320K/320K	40K/40K	40K/40K
IQM	320K/320K	40K/40K	40K/40K
ICR	160K/160K	20K/20K	20K/20K
IQR	160K/160K	20K/20K	20K/20K
Flickr30k-CNA	29.7K/148.9K	1K/5K	1K/5K

## D More Cases about Entity-conditioned Image Visualization

In this experiment, we provide more cases of image visualization given an entity. From Figure D, our proposed R2D2 is able to align the entities with patches of images. Especially, R2D2 has the ability to capture the salient areas when given an image with complex backgrounds, such as the images of “A train” and “A bull”. Our R2D2 also precisely locates different objects within the same image, as shown in the images of “A cup of yogurt” and “Banana”. Moreover, we analyze some bad cases in Figure E. We find that the attention score is disturbed when two adjacent entities are present in an image. This phenomenon is particularly evident for objects with similar colors or categories.



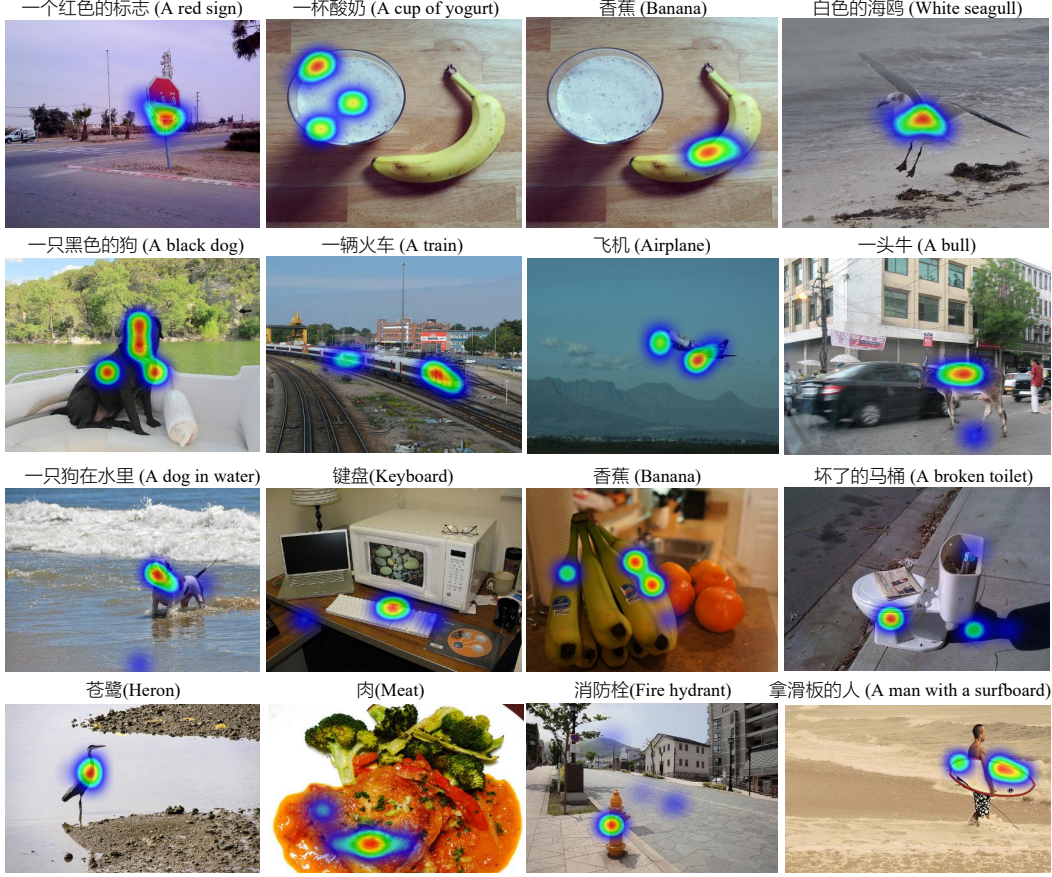


Figure D: More Examples of entity-conditioned image visualization.

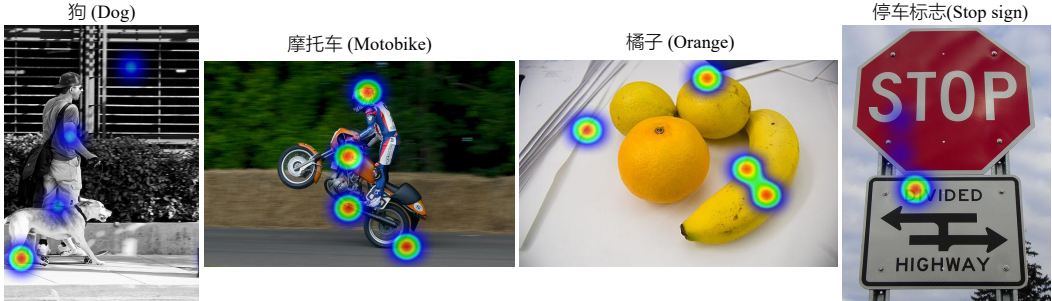


Figure E: Bad cases of entity-conditioned image visualization.

## E Further Results on the Test Set of Flickr30k-CNA

For a fair comparison, we conduct the above experiments on the test set of Flickr30k-CN in the main paper. Especially, we also re-translate the test set of Flickr30k via professional English and Chinese linguists. To demonstrate the superiority of our translated test set, we compare different fine-tuned models of R2D2 under the same pre-trained model on the test set of Flickr30k-CNA.

To be specific, we use the models fine-tuned on the training data of Flickr30k-CN and Flickr30k-CNA, respectively. From Table B, R2D2 trained with Flickr30k-CNA achieves a significant improvement. From the first row of Table B, we get a 0.9% improvement on R@M. When we use the test set of Flickr30k-CN, the gap is only 0.5% (92.2 VS 92.7), as shown in Table 2 in the main paper. This implies that our annotated high-quality data is more valuable when evaluating model capabilities.

Table B: The performance on the test set of Flickr30k-CNA with different training set.

Method	# Pre-train Pairs	Training Set	Image-to-Text Retrieval			Text-to-Image Retrieval			R@M
			R@1	R@5	R@10	R@1	R@5	R@10	
R2D2 <sub>ViT-B</sub>	2.3M	Flickr30k-CN	88.9	98.9	99.6	75.1	93.3	96.2	92.0
		Flickr30k-CNA	90.6	99.4	99.7	77.0	94.3	96.6	<b>92.9</b>
R2D2 <sub>ViT-B</sub>	23M	Flickr30k-CN	92.2	99.2	99.9	78.5	94.4	97.0	93.5
		Flickr30k-CNA	92.9	99.4	99.7	80.2	95.1	97.4	<b>94.1</b>
R2D2 <sub>ViT-L</sub>	2.3M	Flickr30k-CN	95.8	99.7	99.9	81.8	96.0	97.6	95.1
		Flickr30k-CNA	96.2	99.8	99.9	82.9	96.2	98.0	<b>95.5</b>
R2D2 <sub>ViT-L</sub>	23M	Flickr30k-CN	96.0	99.8	100.0	83.8	96.2	97.9	95.6
		Flickr30k-CNA	96.6	99.7	99.9	84.8	96.8	98.3	<b>96.0</b>
R2D2 <sub>ViT-L</sub>	250M	Flickr30k-CN	96.3	99.7	99.9	85.0	96.8	98.6	96.1
		Flickr30k-CNA	97.0	99.8	100.0	85.9	97.4	98.8	<b>96.5</b>